CHIN. PHYS. LETT. Vol. 36, No. 6 (2019) 067101

First-Principles Investigation on the Fully Compensated Ferrimagnetic Behavior in Ti_2NbSb and TiZrNbSb *

Lin Feng(冯琳)**, Xue-Ying Zhang(张雪颖)

Department of Physics, Taiyuan University of Technology, Taiyuan 030024

(Received 15 January 2019)

The electronic structures of Ti_2NbSb with Hg_2CuTi structure and TiZrNbSb with LiMgPdSn structure are investigated using first-principles calculations. The results indicate that Ti_2NbSb is a fully compensated ferrimagnetic spin-gapless semiconductor with an energy gap of 0.13 eV, and TiZrNbSb is a half-metallic fully compensated ferrimagnet with a half-metallic gap of 0.17 eV. For Ti_2NbSb, the total energy of the Hg_2CuTi structure is 0.62 eV/f.u. higher than that of the $L2_1$ structure, which is the ground state, and for TiZrNbSb, the total energy of the structure considered in this work is only 0.15 eV/f.u. larger than that of the ground state. Thus both of them may be good candidates for spintronic applications.

PACS: 71.15.Mb, 71.20.Be, 71.20.−b DOI: 10.1088/0256-307X/36/6/067101

Heusler-type magnetic compounds show very extensive physical properties, for example, the magnetostriction effect,[1] magnetic-induced shape memory effect,[2] magnetoresistance effect,[3] magnetocaloric effect,[4] and exchange bias effect.[5] Thus these compounds have a wide range of applications in industrial production and daily life. The exploration and development of new-type Heusler magnetic compounds have always been a hot topic in the field of magnetic functional materials. Among these magnetic materials, the fully compensated ferrimagnet (FCF), whose total magnetic moment is zero, has drawn great interest from the magnetic electronic industry due to the fact that the almost-zero stray field leads to a very small energy loss. On the other hand, the half-metal properties have been extensively investigated for their 100% spin polarization, which could be used in spintronic applications. Recently, the large anomalous Hall effect has been found in $Co_3Sn_2S_2$,[6,7] which is not only a half-metal, but also a magnetic Weyl semimetal. The large anomalous Hall effect has also been predicted in Ti_2MnAl,[8] which is also a fully compensated ferrimagnet. In addition, the half-metallic FCF (HM-FCF), which was first proposed and investigated by Leuken and de Groot,[9] has attracted great interest recently. Compared with traditional half-metals, HM-FCFs have the following advantages:[10,11] (i) these kind of materials generally has a high Curie temperature; (ii) their responses to the external magnetic field are not sensitive; and (iii) they have a very small energy loss due to the zero net magnetic moment. To date, many Heusler compounds have been predicted to be HM-FCFs, including Mn_3Ga,[12] Cr_2MnZ (Z=P, As, Sb, Bi),[13] Cr_2YZ (Y=Co, Fe; Z=Al, Ga, In, Si, Ge, Sn),[14] Cr_2CoGa,[15] Mn_2Sn,[16] and so on. Recently, $Mn_2Ru_{0.5}Ga$[17] and $Mn_{1.5}V_{0.5}FeAl$[18] have been experimentally confirmed to be HM-FCFs.

In addition, the FCF spin-gapless semiconductor (FCF-SGS) is also very useful in the spintronic field. For an SGS, the energy gap in one of the spin channels is zero, while that in the other spin channel is considerable. This special electronic structure gives rise to a carrier mobility much higher than that in normal semiconductors. Furthermore, a zero energy gap means that the electrons can be excited from the valence band to the conduction band without extra energy. Thus SGSs can show many extraordinary properties,[19] such as a conductance nearly independent of the temperature, a high resistance accompanied with a high magnetic transition temperature, and an almost zero Seebeck coefficient. In addition, FCF-SGSs have the advantages of SGS and FCF at the same time and have a wider application than SGSs in the spintronic field. Up to now, many compounds have been predicted to be FCF-SGSs, such as Mn_2Si,[20] Cr_2ZnZ (Z=Si, Ge, Sn),[21] Ti_2CrSi,[22] Zr_2MnZ (Z=Al, Ga, In),[23] V_3Al,[24] CrVCaP,[25] and CrVTiAl,[26]. However, up to now, experimental evidence of FCF-SGS has only been observed in V_3Al[24] and CrVTiAl.[26]

It is well known that the electronic structure of many Heusler compounds can usually be predicted based on the number of valence electrons.[27] Many studies indicate that Heusler compounds with the valence electrons of 18 or 28 are most likely to be FCF-SGSs.[11,20,21,25] Thus, according to this principle, we speculate that Ti_2NbSb and TiZrNbSb, which have 18 valence electrons, may be suitable FCF-SGS candidates. In this work, we have investigated the electronic structure of Ti_2NbSb with Hg_2CuTi structure and TiZrNbSb with LiMgPdSn structure using first-principles calculations. The calculated results indicate that Ti_2NbSb is an FCF-SGS and TiZrNbSb is an HM-FCF.

The CASTEP code[28] based on the density

*Supported by the National Natural Science Foundation of China under Grant No 51301119, the Natural Science Foundation for Young Scientists of Shanxi Province under Grant No 2013021010-1, and the Scientific and Technological Innovation Programs of Higher Education Institutions of Shanxi Province under Grant No 201802023.

**Corresponding author. Email: fenglin@tyut.edu.cn

© 2019 Chinese Physical Society and IOP Publishing Ltd

functional theory has been employed to investigate Ti_2NbSb and TiZrNbSb. The Perdew, Burke and Ernzerhof[29] parametered generalized gradient approximation[30] has been used to describe the exchange-correlation energy. The interaction between ion core and valence electrons is treated by the ultrasoft pseudo-potential.[31] The electronic configurations with core-level correction are Ti ($3d^2 4s^2$), Nb ($4d^4 5s^1$), Zr ($4d^2 5s^2$), and Sb ($5s^2 5p^3$), respectively. The cut-off energy of the plane wave basis set is 400 eV for all cases. The standard of convergence for the calculations is set as the total energy difference within 10^{-6} eV/atom. The irreducible Brillouin region is divided into 120 k-points ($15 \times 15 \times 15$) following the Monkhorst–Pack method.[32] For the geometry optimization process, the convergence tolerances for energy, force, displacement of a single atom, and internal stress are 10^{-6} eV/atom, 0.01 eV/Å, 5.0×10^{-4} Å, and 2.0×10^{-2} GPa, respectively.

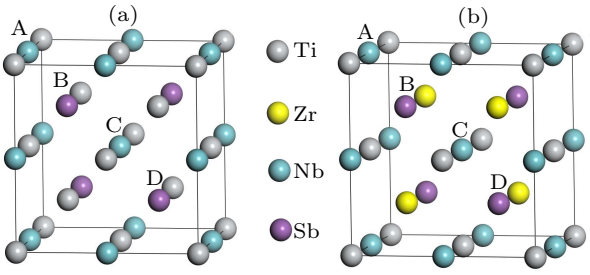

Fig. 1. Atomic configurations of (a) Ti_2NbSb with the Hg_2CuTi structure and (b) TiZrNbSb with the LiMgPdSn structure.

Heusler compounds are generally represented by the formula X_2YZ, in which X and Y are transition metal elements and Z is a main group element. The structure is composed of four interpenetrating fcc lattices, and A, B, C, and D atoms occupy (0, 0, 0), (0.25, 0.25, 0.25), (0.5, 0.5, 0.5), and (0.75, 0.75, 0.75), respectively, in Wyckoff coordinates. When half the X atoms are replaced by X′ atoms, the quaternary Heusler compound XX′YZ is obtained. Generally speaking, for Heusler alloys, the transition metal atoms with more valence electrons tend to occupy A and C sites, while the transition metal atoms with less valence electrons tend to occupy B sites, and the main group atoms tend to occupy D sites. According to this occupying principle, Ti_2NbSb and TiZrNbSb should have formed the Hg_2CuTi and LiMgPdSn structures, respectively. To test this principle, we searched for the stable crystal structure of Ti_2NbSb and TiZrNbSb by geometry optimization. During the geometry optimization process, the non-magnetic state, ferromagnetic state, and antiferromagnetic state are all considered. It was found that for these two compounds, this rule is not valid. We find that the ground state of Ti_2NbSb is an $L2_1$ structure ($Fm\bar{3}m$, space group No. 225), which does not show any magnetism. Further calculations indicate that, for Ti_2NbSb, the total energy of the Hg_2CuTi structure ($F\bar{4}3m$, space group No. 216) is 0.62 eV/f.u. higher than that of the $L2_1$ structure. This value is relatively large as an energy difference between two structures of the same compound, which means that Ti_2NbSb with Hg_2CuTi structure may be difficult to obtain in the experiment. However, the electronic structure of the Hg_2CuTi structure is very special and worth studying. Thus in this study, the Hg_2CuTi structure of Ti_2NbSb conforming to the above occupying principle is considered (as shown in Fig. 1(a)), in which Ti atoms occupy A (0, 0, 0) and B (1/4, 1/4, 1/4) sites, and Nb and Sb atoms occupy C (1/2, 1/2, 1/2) and D (3/4, 3/4, 3/4) sites, respectively. The obtained lattice parameter of Ti_2NbSb is $a = 6.63$ Å. For TiZrNbSb, we find that the ground state is a LiMgPdSn structure ($F\bar{4}3m$, space group No. 216), in which Ti and Zr atoms occupy A (0, 0, 0) and C (1/2, 1/2, 1/2) sites, while Nb and Sb atoms occupy B (1/4, 1/4, 1/4) and D (3/4, 3/4, 3/4) sites, respectively. Here it should be noted that this structure is not the LiMgPdSn structure predicted by the above occupying principle. In addition, this ground state is paramagnetic and its electronic structure is plain. Here another LiMgPdSn structure conforming to the above occupying principle (as shown in Fig. 1(b)) is considered, in which Ti and Zr atoms occupy A (0, 0, 0) and B (1/4, 1/4, 1/4) sites, while Nb and Sb atoms occupy C (1/2, 1/2, 1/2) and D (3/4, 3/4, 3/4) sites, respectively. Its total energy is only 0.15 eV/f.u. larger than the ground state and its electronic structure is extraordinary. Thus the following discussion on TiZrNbSb is based on this LiMgPdSn structure, and the obtained lattice parameter of TiZrNbSb is $a = 6.75$ Å.

Table 1. Total magnetic moment in μ_B (M_T), atomic magnetic moment in μ_B ($M_{Ti(A)}$, $M_{Ti(B)/Zr}$, M_{Nb}, and M_{Sb}), band gap energy in the spin-up channel (E_{up}), and band gap energy in the spin-down channel (E_{down}). The unit of energy is eV.

Compound	M_T	$M_{Ti(A)}$	$M_{Ti(B)/Zr}$	M_{Nb}	M_{Sb}	E_{up}	E_{down}
Ti_2NbSb	0.05	1.16	0.16	−1.28	0.02	0.00	0.13
TiZrNbSb	−0.02	1.02	0.04	−1.12	0.02		0.34

Figure 2 shows the total and partial densities of states (DOS) of Ti_2NbSb. It can be found that the Fermi level locates in a zero energy gap in the spin-up channel, indicating a gapless semiconductor characteristic. On the other hand, the Fermi level falls just on the right in a small gap (0.13 eV) in the spin-down channel, indicating a semiconductor characteristic. The band structure of Ti_2NbSb is shown in Fig. 3. We can find that the energy gap in the spin-up channel is indirect (from W to L) and the energy gap in the spin-down channel is also indirect (from G to L). In addition, the total magnetic moment of Ti_2NbSb is almost zero ($0.05\mu_B$). The magnetic moments of Ti(A) and Ti(B) are $1.16\mu_B$ and $0.16\mu_B$, respectively, while

the magnetic moments of Nb and Sb are $-1.28\mu_B$ and $0.02\mu_B$, respectively. Thus Ti_2NbSb is an FCF-SGS.

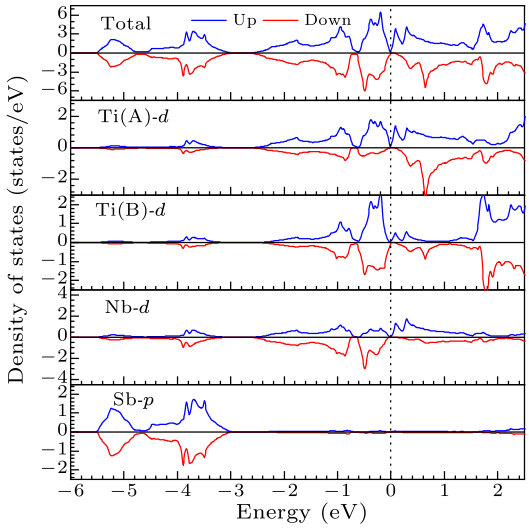

Fig. 2. DOS of Ti_2NbSb.

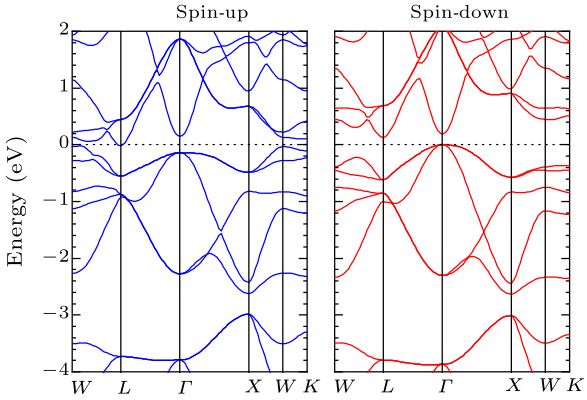

Fig. 3. Band structure of Ti_2NbSb.

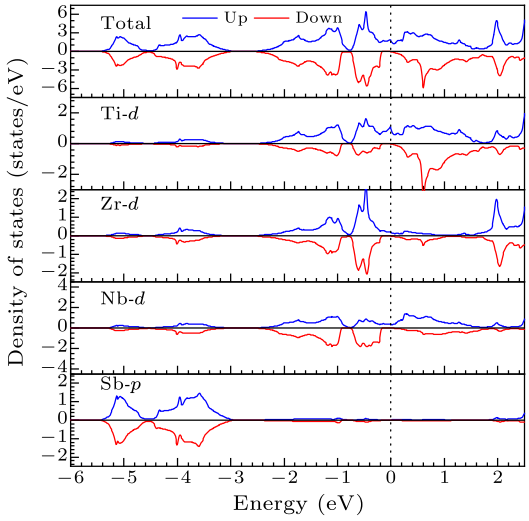

Fig. 4. DOS of TiZrNbSb.

Figure 4 shows the total and partial DOS of TiZrNbSb. It can be found that the Fermi level is located in an energy band in the spin-up channel, indicating a metal characteristic. On the other hand, the Fermi level falls just to the right in a small gap (0.34 eV) in the spin-down channel, indicating a semiconductor characteristic. The band structure of TiZrNbSb is shown in Fig. 5. We can find that the energy gap in the spin-down channel is indirect. In addition, the total magnetic moment of TiZrNbSb is almost zero ($-0.02\mu_B$). The magnetic moments of Ti and Zr are $1.02\mu_B$ and $0.04\mu_B$, respectively, while the magnetic moments of Nb and Sb are $-1.12\mu_B$ and $0.02\mu_B$, respectively. Thus TiZrNbSb is an HM-FCF. Its half-metallic gap is 0.17 eV. Here the half-metallic gap is determined as the minimum between the bottom energy of the conduction bands in the spin-down (up) channel with respect to the Fermi level and the absolute values of the top energy of the valence bands in the spin-down (up) channel. The larger the half-metallic gap, the more stable it is for the material to be used in practical application. In addition, the linear band crossing in the spin-up channel along the W–L path indicates that there may be Weyl nodes around this path in the Brillouin zone, which may lead to a large anomalous Hall effect. We will carry out a further study of this phenomenon in the future.

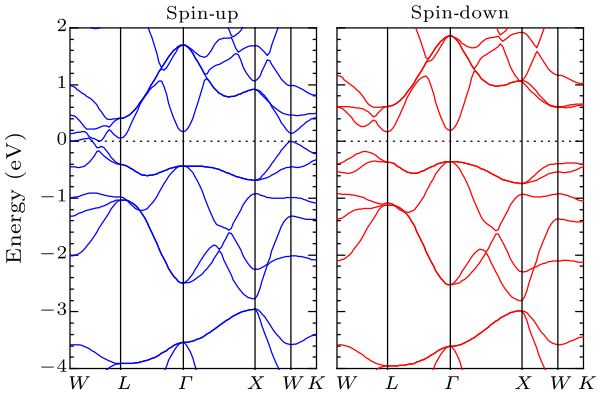

Fig. 5. Band structure of TiZrNbSb.

To understand the atomic hybridization and the role of each atom, the total and partial DOS are further analyzed. For Ti_2NbSb, it can be found that the Sb 5p states are mainly distributed in the range from -6 to -3 eV, which are far away from the Fermi level. The total DOS in the vicinity of the Fermi level is mostly contributed by the Ti(A) 3d, Ti(B) 3d, and Nb 4d states. In the spin-up channel, the states are mostly occupied by Ti(A) 3d electrons and Ti(B) 3d electrons, which are hybridized with each other. In the spin-down channel, there are local and non-hybridized states located at about 0.5 eV above the Fermi level, which mostly originate from Ti(A) 3d states; Ti(B) 3d and Nb 4d states are mainly hybridized with each other below the Fermi level. Thus in the spin-down channel, the bonding hybrids are localized mainly at the Ti(B) and Nb atoms whereas the non-bonding states are mainly at the Ti(A) atoms. The covalent hybridization between the d states of the Ti(A), Ti(B), and Nb atoms gives rise to the gap in the spin-down channel, which is the energy interval between bonding

and non-bonding bands.[33] On the other hand, it can be found that the atomic hybridization in TiZrNbSb is very similar to that in Ti_2NbSb, and Zr plays the role of Ti(B) in Ti_2NbSb.

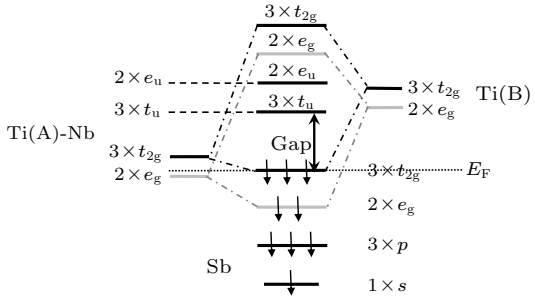

Fig. 6. Diagrammatic sketch of the hybridization of Ti_2NbSb.

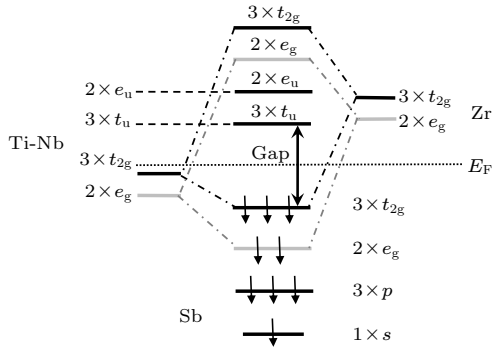

Fig. 7. Diagrammatic sketch of the hybridization of TiZrNbSb.

We present the diagrammatic sketches for the hybridizations of Ti_2NbSb and TiZrNbSb in the spin-down channel in Figs. 6 and 7, based on the above analysis on the atomic hybridization. For Ti_2NbSb, due to the fact that Ti(A) and Nb occupy A and C sites, respectively, which are equivalent from the viewpoint of crystal symmetry, there is a hybridization between their d orbitals with the same symmetry. After the hybridization, five bonding states (double-degenerate e_g and triple-degenerate t_{2g}) and five non-bonding states (triple-degenerate t_u and double-degenerate e_u) are formed. These bonding states further hybridize with the d orbitals of the nearest neighboring Ti(B) while the non-bonding states keep the original pattern.

The situation in TiZrNbSb is similar to that in Ti_2NbSb, and the difference is that Zr in TiZrNbSb plays the role of Ti(B) in Ti_2NbSb. Thus there are nine occupied states in each of the two spin directions ($1\times s$, $3\times p$, $3\times t_{2g}$, and $2\times e_g$), and the total magnetic moment of the compounds should follow the Slater–Pauling rule with $M_t = N_v - 18$,[34] where M_t is the total magnetic moment (in μ_B/f.u.) and N_v is the total number of valence electrons. Since both the numbers of valence electrons of Ti_2NbSb and TiZrNbSb are 18, both of their total magnetic moments are zero. In addition, both the gaps of Ti_2NbSb and TiZrNbSb are determined by the energy interval between the bonding t_{2g} states and the non-bonding t_u states. For Ti_2NbSb, the Fermi level is located at the top of the bonding t_{2g} states, while the Fermi level lies in the band gap in TiZrNbSb. This may be due to the fact that the atomic mass of Zr is greater than that of Ti, and the hybridization becomes stronger in TiZrNbSb, giving rise to a larger band gap. In addition, the hybridization for Ti_2NbSb in the spin-up channel is the same as that in the spin-down channel. Due to the fact that the bonding t_{2g} states just touch the non-bonding t_u states, the energy interval between them is just zero, and a zero-gap appears in the spin-up channel.

In summary, the electronic structure and magnetic properties of Ti_2NbSb with Hg_2CuTi structure and TiZrNbSb with LiMgPdSn structure have been investigated using first-principles calculations. The calculated results indicate that Hg_2CuTi-type Ti_2NbSb is an FCF-SGS, and its energy gap in the spin-up channel is zero, while that in the spin-down channel is 0.13 eV. LiMgPdSn-type TiZrNbSb is an HM-FCF, and its half-metallic gap is 0.17 eV. Further analysis shows that their energy gaps in the spin-down channel originate from the energy interval between the bonding t_{2g} states and the non-bonding t_{1u} states. Their magnetic moments follow the Slater–Pauling rule with $M_t = N_v - 18$. Thus Hg_2CuTi-type Ti_2NbSb and LiMgPdSn-type TiZrNbSb may be good candidates for spintronic applications.

References

[1] Ullakko K, Huang J K, Kantner C, O'Handley R C and Kokorin V V 1996 *Appl. Phys. Lett.* **69** 1966
[2] Kainuma R, Imano Y, Ito W, Sutou Y, Morito H, Okamoto S, Kitakami O, Oikawa K, Fujita A, Kanomata T and Ishida K 2006 *Nature* **439** 957
[3] Yu S Y, Liu Z H, Liu G D, Chen J L, Cao Z X, Wu G H, Zhang B and Zhang X X 2006 *Appl. Phys. Lett.* **89** 162503
[4] Liu J, Gottschall T, Skokov K P, Moore J D and Gutfleisch O 2012 *Nat. Mater.* **11** 620
[5] Wang B M, Liu Y, Ren P, Xia B, Ruan K B, Yi J B, Ding J, Li X G and Wang L 2011 *Phys. Rev. Lett.* **106** 077203
[6] Liu E K, Sun Y, Kumar N, Muechler L, Sun A L, Jiao L, Yang S Y, Liu D F, Liang A J, Xu Q N, Kroder J, Süß V, Borrmann H, Shekhar C, Wang Z S, Xi C Y, Wang W H, Schnelle W, Wirth S, Chen Y L, Goennenwein S T B and Felser C 2018 *Nat. Phys.* **14** 1125
[7] Wang Q, Xu Y F, Lou R, Liu Z H, Li M, Huang Y B, Shen D W, Weng H M, Wang S C and Lei H C 2018 *Nat. Commun.* **9** 3681
[8] Shi W J, Muechler L, Manna K, Zhang Y, Koepernik K, Car R, van den Brink J, Felser C and Sun Y 2018 *Phys. Rev. B* **97** 060406
[9] Leuken H V and de Groot R 1995 *Phys. Rev. Lett.* **74** 1171
[10] Galanakis I, Özdoğan K, Şaşıoğlu E and Aktaş B 2007 *Phys. Rev. B* **75** 092407
[11] Wang X T, Cheng Z X, Wang J L, Wang X L and Liu G D 2016 *J. Mater. Chem. C* **4** 7176
[12] Wurmehl S, Kandpal H C, Fecher G H and Felser C 2006 *J. Phys.: Condens. Matter* **18** 6171
[13] Galanakis I, Özdoğan K, Şaşıoğlu E and Aktaş B 2007 *Phys. Rev. B* **75** 172405
[14] Meinert M and Geisler M P 2013 *J. Magn. Magn. Mater.* **341** 72
[15] Galanakis I and Şaşıoğlu E 2011 *Appl. Phys. Lett.* **99** 052509

[16] Luo H Z, Liu G D, Meng F B, Wang W H, Wu G H, Zhu X X and Jiang C B 2011 *Physica B* **406** 4245
[17] Kurt H, Rode K, Stamenov P, Venkatesan M, Lau Y C, Fonda E and Coey J M D 2014 *Phys. Rev. Lett.* **112** 027201
[18] Stinshoff R, Nayak A K, Fecher G H, Balke B, Ouardi S, Skourski Y, Nakamura T and Felser C 2017 *Phys. Rev. B* **95** 060410(R)
[19] Ouardi S, Fecher G H, Felser C and Kübler J 2013 *Phys. Rev. Lett.* **110** 100401
[20] Zhang Y J, Liu Z H, Liu G D and Ma X Q 2015 *J. Magn. Magn. Mater.* **387** 67
[21] Zhang Y J, Liu Z H, Liu E K, Liu G D, Ma X Q and Wu G H 2015 *Europhys. Lett.* **111** 37009
[22] Wang L and Jin Y J 2015 *J. Magn. Magn. Mater.* **385** 55
[23] Birsan A and Kuncser V 2016 *J. Magn. Magn. Mater.* **406** 282
[24] Jamer M E, Assaf B A, Sterbinsky G E, Arena D, Lewis L H, Saul A A, Radtke G and Heiman D 2015 *Phys. Rev. B* **91** 094409
[25] Özdoğan K, Şaşıoğlu E and Galanakis I 2015 *Comput. Mater. Sci.* **110** 77
[26] Venkateswara Y, Gupta S, Samatham S S, Varma M R, Enamullah, Suresh K G and Alam A 2018 *Phys. Rev. B* **97** 054407
[27] Graf T, Felser C and Parkin S S P 2011 *Prog. Solid State Chem.* **39** 1
[28] Clark S J, Segall M D, Pickard C J, Hasnip P J, Probert M I J, Refson K and Payne M C 2005 *Z. Kristallogr.* **220** 567
[29] Perdew J P, Burke K and Ernzerhof M 1996 *Phys. Rev. Lett.* **77** 3865
[30] Perdew J P, Chevary J A, Vosko S H, Jackson K A, Pederson M R, Singh D J and Fiolhais C 1992 *Phys. Rev. B* **46** 6671
[31] Vanderbilt D 1990 *Phys. Rev. B* **41** 7892
[32] Monkhorst H J and Pack J D 1976 *Phys. Rev. B* **13** 5188
[33] Galanakis I, Dederichs P H and Papanikolaou N 2002 *Phys. Rev. B* **66** 134428
[34] Galanakis I, Mavropoulos P and Dederichs P H 2006 *J. Phys. D* **39** 765